Available online at www.sciencedirect.com
SCIENCE DIRECT®
Physica A 321 (2003) 59–70
PHYSICA A
www.elsevier.com/locate/physa

Conformal invariance and simulations in curved geometries

Henk W.J. Blöte[a,b,*], Youjin Deng[a]

[a] *Faculty of Applied Sciences, P.O. Box 5046, 2600 GA Delft, The Netherlands*
[b] *Instituut Lorentz, Universiteit Leiden, Postbus 9506, 2300 RA Leiden, The Netherlands*

Abstract

Conformal mappings serve as useful tools for the determination of universal properties of critical models. Typical applications are subject to a major restriction, namely that the pertinent conformal mapping should lead to a geometry that can be investigated by means of numerical methods such as Monte Carlo simulations. Since conformal mappings of 3-D systems usually lead to curved geometries which are difficult to investigate numerically, most applications have thus far been restricted to 2-D systems. We present a solution of this problem for discrete spin models, by taking the anisotropic or Hamiltonian limit which renders one of the lattice directions continuous, such that the dimensionality in effect reduces by one. Applications to the 3-D Ising and percolation models confirm the predictions obtained from the assumption of conformal invariance, and lead to accurate numerical results for the scaling dimensions.

PACS: 05.50.+q; 64.60.Cn; 64.60.Fr; 75.10.Hk

Keywords: Critical phenomena; Conformal invariance; Monte Carlo methods

1. Introduction

The theory of conformal invariance has provided considerable fundamental insight in critical phenomena by predicting spectra of critical exponents in two-dimensional models [1–3]. Other interesting theoretical results follow from conformal mappings of correlation functions between models defined in different geometries. A well-known, and particularly useful example is Cardy's mapping [4] between an infinite plane and the surface of a cylinder. This conformal mapping relates the power of the algebraic

* Corresponding author.
E-mail address: henk@tntnhbn.tn.tudelft.nl (H.W.J. Blöte).

0378-4371/03/$ - see front matter
doi:10.1016/S0378-4371(02)01752-1

decay of correlations in the infinite plane to the characteristic length of the exponentially decaying correlation functions along a cylinder. On this basis one can obtain in a, from a technical point of view, relatively simple way the scaling dimensions from the eigenvalues of the transfer matrix of the model wrapped on the cylinder, or in other words, on a flat strip with periodic boundary conditions.

The conformal mapping between the infinite plane and the surface of a cylinder can be generalized to more dimensions [5]. We recall the mapping for the case of three dimensions. As a first step the Cartesian coordinates (x, y, z) are rewritten as spherical coordinates (r, θ, φ). While these coordinates still describe a flat space, the nonlinearity of the transformation modifies the metric tensor, as expressed by the invariant line element which reads

$$\mathrm{d}s^2 = \mathrm{d}x^2 + \mathrm{d}y^2 + \mathrm{d}z^2 \,, \tag{1}$$

in Cartesian coordinates and

$$\mathrm{d}s^2 = \mathrm{d}r^2 + r^2 \ (\mathrm{d}\theta^2 + \sin^2\theta \, \mathrm{d}\varphi^2) \tag{2}$$

in spherical coordinates. We specify the conformal mapping by

$$(r, \theta, \varphi) \to (u, \theta, \varphi) \quad \text{with} \quad u = R \log r \,. \tag{3}$$

Expressed in the new coordinates, the line element Eq. (2) becomes

$$\mathrm{d}s^2 = R^{-2} \mathrm{e}^{2u/R} [\mathrm{d}u^2 + R^2 \ (\mathrm{d}\theta^2 + \sin^2\theta \, \mathrm{d}\varphi^2)] \,, \tag{4}$$

where R is a free parameter of the transformation. But here we adopt instead a metric described by a line element $\mathrm{d}s'$ according to

$$\mathrm{d}s'^2 = [\mathrm{d}u^2 + R^2 \ (\mathrm{d}\theta^2 + \sin^2\theta \, \mathrm{d}\varphi^2)] \,. \tag{5}$$

The mapping is conformal because the line elements $\mathrm{d}s$ and $\mathrm{d}s'$ differ only by a position-dependent factor. The new metric describes a 3-D space in which two coordinates (θ, φ) parametrize the surface of a sphere while the third coordinate u specifies a direction perpendicular to the surface of the sphere: the contributions of $\mathrm{d}u$ to the line element are independent of θ and φ, and those of $\mathrm{d}\theta$ and $\mathrm{d}\varphi$ are independent of u. Since the range $-\infty < u < \infty$ is unbounded, while θ and φ are restricted to a finite range, the new space is finite in two directions and infinite in the third. The analogy with a 2-D cylinder is obvious; the cylindrical geometry can be algebraically characterized as $S^1 \times \mathbb{R}^1$, where S^1 represents a cyclic number (circle) and $\mathbb{R}$ the real numbers (infinite line). The 3-D geometry described by Eq. (5) can be characterized as $S^2 \times \mathbb{R}^1$: the difference with the 2-D case is that the circle (S^1) is now replaced by a sphere (S^2). Thus one can refer to the space $S^2 \times \mathbb{R}^1$ as a 'spherocylinder'. There is however an important difference between the 2-D and 3-D cases. Unlike the 2-D case, where the net curvature is zero, the spherocylinder has a net curvature as implied by Eq. (5).

Therefore, it is not surprising that applications of the conformal mapping Eqs. (3) and (5) are very scarce. A numerical finite-size analysis of a model on a spherocylinder might be achieved by placing a sequence of regular lattices in this geometry, but this is obviously a difficult problem. The linear u-direction can simply be discretized, so that

the problem reduces to placing regular 2-dimensional lattices on a sphere. However, the spherical coordinates θ and φ seem to defy any acceptable discretizations. Cardy [5] avoided this problem for the special case of the spherical model, thereby disposing of the discrete lattice structure. Weigel and Janke [6] approximated the surface S^2 of the sphere by that of a cube. They numerically investigated Ising models in this 3-D geometry by means of Monte Carlo simulations, and concluded that the above-mentioned relation between scaling dimensions and correlation lengths is still satisfied, provided a constant factor is included. Apparently this factor accounts for the different shapes of the sphere and the cube.

We have developed a technique that enables the simulation of discrete spin models in curved spaces. This technique involves two steps; the first one is to take the anisotropic, or Hamiltonian limit of the lattice model. This in effect eliminates the lattice structure in one direction; arrays of spins are replaced by continuous lines of spins. The dimensionality, in a sense, decreases by 1. This solves a part of the problem of the definition of a model in a curved space. The remaining part of the problem may be solved by a suitable choice of the coordinate system of the anisotropic model in the curved space. For instance, on the surface of a sphere we may represent the lattice structure by a series of coaxial circles. The second step of our technique involves the formulation of a cluster Monte Carlo algorithm for the Hamiltonian limit. The algorithm is of the Wolff cluster type and thus suppresses critical-slowing down. It has an efficiency of the same order as the Wolff algorithm for a model with equal couplings in the three spatial directions. In Section 2 we review the anisotropic limit of the Ising model and its relation with the transverse Ising model. Section 3 describes the cluster algorithm for the anisotropic limit, using the language of the Ising model. It thus applies to the transverse Ising model. Trivial modifications generalize it to the Hamiltonian limit of Potts models, including the percolation model. Section 4 illustrates the use of the algorithm by means of briefly summarized applications to the 3-D Ising and percolation models on a spherocylinder. A short conclusion is given in Section 5.

2. The anisotropic limit of the Ising model

The 3-D Ising model with anisotropic couplings is described by the Hamiltonian

$$\mathscr{H}/k_{\mathrm{B}}T = -\sum_{x,\,y,\,z} [K_{xy} s_{x,y,z}(s_{x+1,y,z} + s_{x,\,y+1,\,z}) + K_z s_{x,y,z} s_{x,y,z+1}] \,, \tag{6}$$

where the integers $1 \leqslant x \leqslant L$, $1 \leqslant y \leqslant L$ and $1 \leqslant z \leqslant L'$ label the sites of a cubic lattice. K_{xy} and K_z are the coupling strengths along bonds perpendicular and parallel to the z direction, respectively. The spins can assume the values $s_{x,y,z} = \pm 1$. Periodic boundary conditions apply. For simplicity we have defined the model such that the x and y directions are equivalent but we allow differences with respect to the z direction. In particular we are interested in the limit that the couplings in the z direction become strong and those in the x and y directions weak. We shall attempt to follow the ratio of the length scales of the correlations in the inequivalent directions, at least in an approximate sense. This can be done by application of the Migdal [7] renormalization

procedure in the z direction, without rescaling the x and y directions. Each bond in the z direction is thus decorated with $n-1$ Ising spins and the bond strength K_{xy} is distributed accordingly between the newly inserted spins. This leads to a new model with a lattice spacing in the z direction that is smaller by a factor n. The approximate renormalization equations imply that if the new couplings satisfy

$$K_{xy}^{(n)} = K_{xy}/n \quad \text{and} \quad \tanh K_z^{(n)} = [\tanh K_z]^{1/n} , \tag{7}$$

it is roughly equivalent with the original system. These considerations do not only yield the approximate locus of the critical line in the (K_{xy}, K_z) plane, they also show that, along the critical line, the lattice spacing in the z direction should be chosen as $1/n$ in order to maintain approximate isotropy of the correlation functions. We thus describe our system by

$$\mathscr{H}'/k_{\mathrm{B}}T = -\sum_{x,y,z'} [K_{xy}^{(n)} s_{x,y,z'}(s_{x+1,y,z'} + s_{x,y+1,z'}) + K_z^{(n)} s_{x,y,z'} s_{x,y,z'+1}] , \tag{8}$$

where x and y are, as above, integers running from 1 to L but the coordinate z' now assumes the values $1/n, 2/n, 3/n, \ldots, L'$. For large n it is clear that $\tanh K_z^{(n)}$ must be close to 1, so that $1 - \tanh K_z^{(n)} \propto 1/n$, with a proportionality constant that, while dependent on K_z, is unknown except that it is of order 1. Therefore, for moderate values of K_{xy} and K_z, we may, without loss of generality take

$$K_{xy}^{(n)} = 1/(tn) \quad \text{and} \quad \mathrm{e}^{2K_z^{(n)}} = n , \tag{9}$$

where t is a temperature-like variable that depends on K_{xy} and K_z. In contrast with the isotropic Hamiltonian (6) with $K_{xy} = K_z = K$, we expect that Eq. (8) will, in general, not lead to isotropic decay of correlations. However, we purport to restore isotropy asymptotically (at large distances) by an additional rescaling

$$z' \to z = z'/a \tag{10}$$

of the z direction by a factor a which remains to be determined (its value at the critical point is listed in Section 3).

It is known that for $n \to \infty$ model (8) is directly related with the 2-D transverse Ising model. This model consists of quantum spins on the square lattice, with nearest-neighbor couplings and an external field:

$$\mathscr{H}_{\mathrm{QM}} = -\sum_{x} [s_{x,y}^z (s_{x+1,y}^z + s_{x,y+1}^z) + t s_{x,y}^x] , \tag{11}$$

where the s^z and s^x are Pauli matrices. By application of the Trotter–Suzuki formula [8,9] to the partition function of Eq. (11) one indeed finds model (8) with couplings as in Eq. (9) where n is the 'Trotter number' which has, strictly speaking, to be taken infinitely large; and L' is to be identified with the inverse temperature of the transverse Ising model.

3. The cluster algorithm

In the construction of a Monte Carlo algorithm for the anisotropic limit we will have to deal with the divergence of n. Since the number of spins is proportional to n, and

the available computer memory is finite, the spin configuration cannot be stored in the usual way. Fortunately, the number of interfaces between ranges of + and − spins along the z direction remains finite when $n \to \infty$. It is sufficient to store the location of these interfaces; the determination of the sign of the spins at an arbitrary location z' then only requires the additional information of the sign of the spins at a given location, say at $z' = 0$.

Our cluster algorithm is based on earlier work and ideas of Swendsen and Wang [10], Wolff [11] and others [12]. In cluster algorithms one distinguishes between 'rigid' and 'flexible' bonds. These two cases are represented by means of a bond variable having the values $b = 1$ and 0, respectively. These bond variables are precisely those occurring in the Kasteleyn–Fortuin [13] random-cluster model. Thus, a bond variable b_{ij} associated with the coupling K between Ising spins s_i and s_j, is equal to 1 (rigid) with a probability $p_r = \delta_{s_i s_j}(1 - \mathrm{e}^{-2K})$. In a simulation, one would normally need one random number per bond to decide whether a bond is rigid. Since the number of bonds is proportional to the divergent Trotter number n, a different approach is necessary.

Thus we write $b_{ij} = \delta_{s_i s_j} c_{ij}$ where the c_{ij} are 'provisional' bond variables equal to 0 or 1. They are independent random variables and the probability that $c_{ij} = 1$ is $(1 - \mathrm{e}^{-2K})$. First we consider the case that $K = K_z$ so that this probability is almost 1 when n is large. The probability that $m - 1$ consecutive provisional bond variables are equal to 1, while the mth variable is equal to 0, is $p_z(m) = (1 - \mathrm{e}^{-2K_z})^{m-1}\mathrm{e}^{-2K_z}$. Thus the cumulative distribution is

$$P_z(m) = \sum_{k=1}^{m} p_z(k) = 1 - (1 - \mathrm{e}^{-2K_z})^m \tag{12}$$

and a stochastic implementation of this process is the following choice for m

$$P_z(m-1) \leqslant X < P_z(m)\,, \tag{13}$$

where X is a uniformly distributed random number in the range $0 < X < 1$. Equivalently we may replace X by $1 - X$ which leads to

$$m - 1 \leqslant \frac{\log X}{\log(1 - \mathrm{e}^{-2K_z})} < m\,. \tag{14}$$

We choose K_z according to Eq. (9) and express the number m of bonds along the z direction in the corresponding physical length $\Delta z' = m/n$:

$$\Delta z' - 1/n \leqslant -\log X < \Delta z' \tag{15}$$

and in the limiting case we simply have $\Delta z' = -\log X$.

In the construction of a Wolff cluster, this means that a range $\Delta z'$ will be included in the cluster, unless an interface occurs within this range; since we then have $\delta_{s_i s_j} = 0$ we also have $b_{ij} = 0$, even if $c_{ij} = 1$.

The cluster growth in the other directions occurs in an analogous but complementary way. We consider a range without an interface along a line of spins in the z direction, and consider the array of bond variables coupling to a line of neighbors in the x or y direction. As above they are decomposed as $b_{ij} = \delta_{s_i s_j} c_{ij}$, and we first focus on the determination of the c_{ij}. Given the weakness of K_{xy} most of the c_{ij} will be 0.

The probability that $m-1$ consecutive variables are 0 and that the mth one is 1 is $p_{xy}(m) = (\mathrm{e}^{-2K_{xy}})^{m-1}(1-\mathrm{e}^{-2K_{xy}})$. Thus the cumulative distribution is

$$P_{xy}(m) = \sum_{k=1}^{m} p_{xy}(k) = 1 - (\mathrm{e}^{-2K_{xy}})^m \tag{16}$$

and a stochastic implementation of this process is to choose m according to

$$P_{xy}(m-1) \leqslant X < P_{xy}(m)\,, \tag{17}$$

where, as before, we may replace X by $1-X$ so that

$$m - 1 \leqslant -\frac{\log X}{2K_{xy}} < m\,. \tag{18}$$

We choose K_{xy} according to Eq. (9) and express the number m of bonds along the z direction in the corresponding physical length $\Delta z' = m/n$:

$$\Delta z' - 1/n \leqslant -(t/2)\log X < \Delta z' \tag{19}$$

and in the limit we have $\Delta z' = -(t/2)\log X$. For the construction of the Wolff cluster, this means that after a distance $\Delta z'$ a neighbor in the x or y direction will be included in the cluster, unless the neighbor spin has the wrong sign, or an interface occurs within the range $\Delta z'$.

Before starting actual applications of this algorithm, we still require a determination of the critical point t_c, and of the rescaling factor a to restore isotropy asymptotically. This work was done by means of finite systems in a flat space as implied by Eqs. (6) and (8) and will be published elsewhere [15]. The results are $t_c = 3.04438 \pm 0.00002$ and $a = 0.8881 \pm 0.0002$.

Since the model is now continuous in the z direction, application of the algorithm in curved geometries become feasible. We consider the case of the spherocylinder. The continuous z direction is chosen to correspond with the spherical coordinate φ. The originally equivalent x and y directions are chosen to correspond with θ and u. The 'lattice structure' in each sphere is thus represented by L evenly distributed circles. In spherical coordinates (θ,φ) the kth circle is given by $\theta = (k-\frac{1}{2})\pi/L$, with $k = 1,2,\ldots,L$. Each circle represents a continuous line of spins, as illustrated in Fig. 1. The determination of the bond probabilities in the weak-coupling direction requires a well-defined length scale. In the θ-direction we face the complication that the length scales along adjacent circles, although proportional to φ, have different prefactors. The prefactor was chosen as corresponding to the length as measured along the circle halfway, that is the circle with $\theta = k\pi/L$ for bonds between the circles with $\theta = k\pi/L$ and $(k-1)\pi/L$. Note that the circles with $k = 1$ as well as with $k = L$ could, in principle, have self-interactions via weak bonds over the poles $\theta = 0$ and π. But these interactions vanish because the circles at $\theta = 0$ and π have a zero length scale. Alternatively the choice $\theta = (k-\frac{1}{2})\pi/L$, with $k = 1,2,\ldots,L$ may be replaced by $\theta = k\pi/L$ with $k = 0,1,2,\ldots,L$. We have investigated both cases by means of Monte Carlo determinations of the magnetic correlation function between opposite sites θ,φ and $\pi-\theta,\pi+\varphi$. However, the latter choice revealed significant deviations from isotropy, which were not observed for the original choice $\theta = (k-\frac{1}{2})\pi/L$.

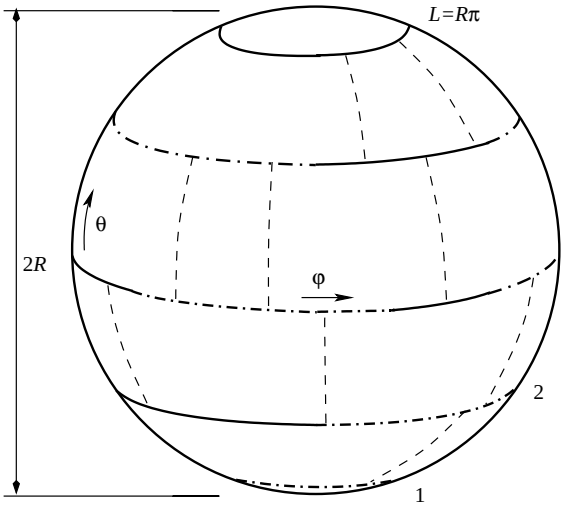

Fig. 1. Intersection S^2 of a spherocylinder with a surface of constant u. It is a sphere, on which $L=5$ circles represent continuous lines of spins in the strong-coupling direction. Weak couplings occur between adjacent circles within spheres as well as between those adjacent in the third dimension (not shown). The full and dash-dotted parts of the circles represent (arbitrarily chosen) ranges of spins with different signs. The dashed lines connecting neighboring circles represent possible random-cluster bonds in the weak-coupling direction.

The presently defined system is rotationally invariant with respect to φ, but the discretization in θ leads to deviations from uniformity. For a finite-size parameter L we may expect a deviation of order L^{-2} in the averaged coupling strength with respect to a flat geometry, in view of the analogy with applications of the trapezium rule. Under renormalization this effect will increase by a factor L^{y_t} where $y_t \approx 1.587$ is the temperature renormalization exponent. Therefore, we expect that this discretization error will lead to finite-size effects of order L^{y_t-2}, which will naturally dominate over the corrections proportional to L^{y_i} where $y_i \approx -0.8$ is the irrelevant exponent.

4. Numerical results

The simulations used the geometry of the spherocylinder described above. The system sizes are taken as L for the number of circles on the sphere (thus the circumference is $2L$) and nL for the physical length in the u direction. To approximate the $S^2 \times \mathbb{R}^1$ geometry we take n as 8. Both periodic and fixed boundary conditions are applied.

4.1. Ising model with periodic boundary conditions

We have simulated systems with periodic boundary conditions in the u direction, and sampled the magnetic and energy–energy correlation functions along the same direction.

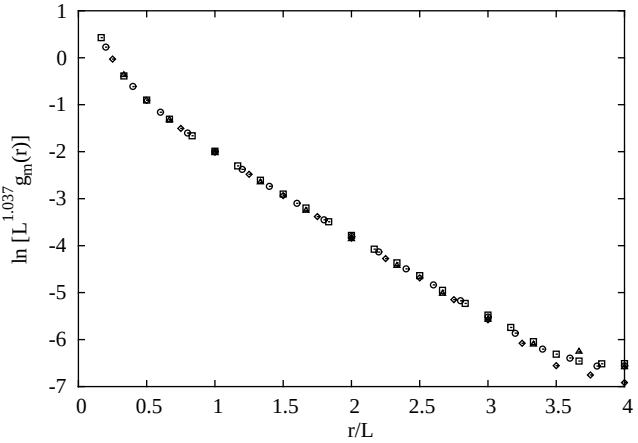

Fig. 2. Data collapse illustrating the exponential decay of the magnetic correlation functions $g_m(r)$ versus distance r. The Monte Carlo data are shown as $\ln[L^{1.037} g_m(r)]$ versus r/L (horizontal), for system sizes $L=6$ (□), $L=8$ (○), $L=10$ (◇) and $L=12$ (△).

Under the conformal transformation (3), the theory of conformal invariance predicts that the two-point correlation functions over a distance r in this direction behave as

$$\langle \sigma(0,\theta,\varphi)\sigma(r,\theta,\varphi)\rangle_{S^2\times\mathbb{R}^1} \propto L^{-2X} \mathrm{e}^{-r/\xi_L}, \quad r \gg 0\,, \tag{20}$$

where σ is a scaling operator such as the magnetization density or the fluctuation of the energy density, X is the corresponding scaling dimension, and $\xi_L \simeq \pi X/L$ is the correlation length in the u direction. Because of the periodic boundary conditions, the correlation functions are built up over two distances r and $4L-r$, and $r \leqslant 4L$.

For the magnetic correlation functions $g_m(r) = \langle m(0)m(r)\rangle$, an example is shown Fig. 2. Because the exponent of L is known to be $-2X \approx -1.037$ (see e.g. Ref. [14]), we achieve a data collapse by taking the vertical scale as $\ln[L^{1.037} g_m(r)]$. The curvature at short distances signals the algebraic decay of the correlation functions for $r < L$, and the upward trend on the right-hand side is due to the periodic image at a distance $4L-r$. The scattering of the data at large distances is due to the large relative statistical uncertainties in this region.

By means of finite-size scaling on the basis of Eq. (20), we analyzed the magnetic- and energy-like correlation lengths, in particular the finite-size amplitude $\xi_L/L \simeq \pi X$. This yields the magnetic and temperature scaling dimensions as $X_h = 0.5178$ (12) and $X_t = 1.423$ (19); these numbers are in a good agreement with the existing results [14,15]. An account of a preliminary analysis, including details on the corrections to scaling that were included, is already in the press [16].

4.2. Ising model with fixed boundary conditions

Here we consider a different conformal transformation. It can conveniently be described in two steps, the first of which is an inversion which maps the 3-D space onto

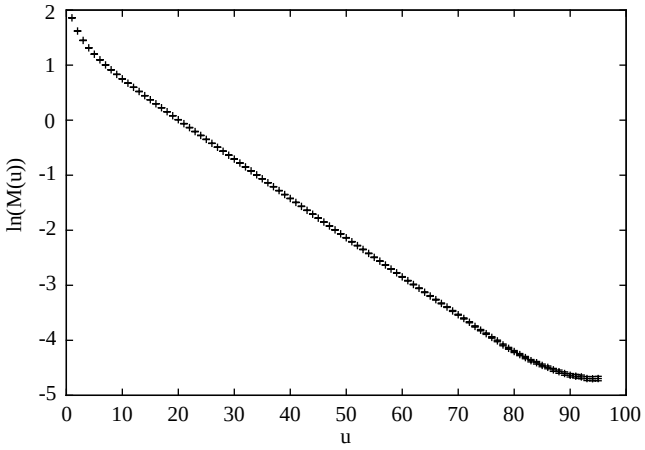

Fig. 3. Exponential decay of the magnetization density $m(u)$ of a system with fixed boundary conditions at $u = 0$, shown as $\ln m(u)$ versus u (horizontal). The system size is $L = 20$. Error bars show the statistical uncertainty.

itself:

$$\mathbf{r}'/r'^2 = \mathbf{r}/r^2 + \hat{\mathbf{R}}'/2 \,, \tag{21}$$

where $\hat{\mathbf{R}}'$ is an arbitrary fixed unit vector at the origin of the primed coordinate system [17]. Under this mapping, the semi-infinite space $\mathbb{R}^2 \times \mathbb{R}^+$ transforms into the interior of a unit sphere. We apply this mapping to a 3-D system with a surface subject to an infinite ordering field. The conformal transformation of the profile of the scaling operator σ in the semi-infinite space leads to the profile of that operator in the unit sphere with fixed boundary conditions at the surface:

$$\langle \sigma(\mathbf{r}') \rangle_{sphere} = A[1 - (r')^2]^{-X_h} \,, \tag{22}$$

where X_h is the corresponding bulk scaling dimension [17]. Under the transformation (3), the interior of this unit sphere is conformally mapped on a semi-infinite spherocylinder, with a surface at $u = 0$ where the sign of the Ising variables is fixed. For such a system, the profile of a scaling operator follows as [15]

$$\langle \sigma(u) \rangle \propto L^{-X_h} \mathrm{e}^{-u/\xi_L} (1 - \mathrm{e}^{-u\pi/2L})^{-X_h} \,. \tag{23}$$

The simulations of these systems used fixed boundary conditions at $u = 0$ and $8L$; the magnetization and energy densities were sampled. Figs. 3 and 4 display examples of these results. In comparison with the corresponding correlation functions, they decay slower as a function of system size L, and the computer time requirements are considerably less [15]. Thus, it seems a promising tool to determine the scaling dimensions. We fitted the Monte Carlo data by means of finite-size scaling on the basis of Eq. (23) but including a correction for the discretization error. The expected deviations at short distances were eliminated by introducing a cutoff at small u. We obtain

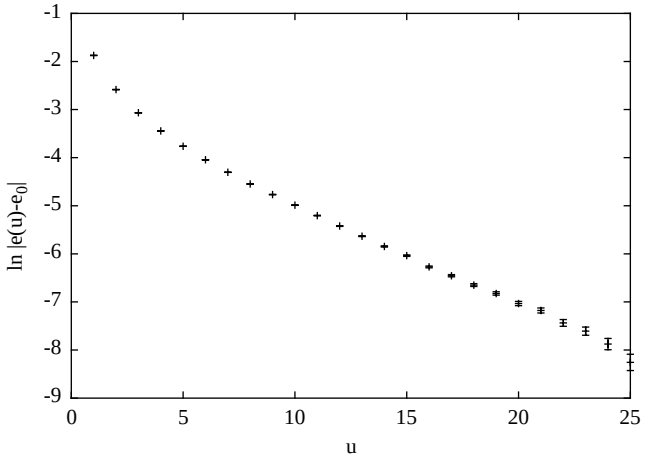

Fig. 4. Exponential decay of the energy density profile $e(u) - e_0$ of a system with fixed boundary conditions at $u = 0$. The data are shown as $\ln|e(u) - e_0|$ versus u (horizontal). The system size is $L = 20$. Error bars show the statistical uncertainty.

$X_h = 0.5186$ (6) and $X_t = 1.414$ (7). The accuracy of the magnetic scaling dimension is comparable to that of the existing results.

4.3. Percolation model with fixed boundary conditions

It is straightforward to apply the cluster algorithm described in Section 3 to Potts models with $q \neq 2$ states, including the bond percolation model with $q = 1$. In the Hamiltonian limit, the bond probabilities are $1 - 1/n$ for the z direction and $2/(tn)$ for the other directions. We used the same anisotropic 3-D geometry as described in Section 3. Analysis of the Monte Carlo data for a flat 3-D geometry leads to the results [15] that the critical point is located at $t_c = 8.6429$ (6), that a rescaling factor $a = 1.5844$ (6) restores asymptotic isotropy of the correlation functions, and that the magnetic critical dimension is $X_h = 0.4783$ (11), etc.

Next, we simulated the bond percolation model on the spherocylinder with fixed boundary conditions in the u direction. We define the quantity $P(u)$ as the probability that a point at position u is connected to the fixed surfaces by any percolating path. The behavior of $P(u)$ in this geometry is expected to be similar to that of the magnetization density (see e.g. Ref. [18]) and thus to be described by Eq. (23), but with a value of X_h that is different from that of the Ising model. We fitted the Monte Carlo data accordingly by means of finite-size scaling, and thus obtained $X_h = 0.4789$ (16) [15], which is in a good agreement with the number mentioned above $X_h = 0.4783$ (11) [15], and with the result of a recent study, namely $X_h = 0.476$ (5) [19].

5. Conclusion

The cluster algorithm appears to be an efficient tool for the investigation of the Hamiltonian limit of discrete Potts models. Its results are in a reasonable qualitative agreement with applications of a recursion of the Migdal type as described in Section 2, which yield $t_c = 3.435$ for the Ising case; shifting bond probabilities in the bond percolation case leads to $t_c = 11.18$. This is in line with the fact that the rescaling factors a are roughly equal to 1 as predicted by the approximation used.

Furthermore the algorithm proves to be suitable for applications in curved geometries such as produced by conformal mappings of systems in a 3-D, flat space. The algorithm may also serve for the investigation of 2-D critical systems in special geometries such as the surface of a sphere or on the interior of a circle.

Concerning the possibility of generalizations to other models, the description of spin configurations by means of well-defined interfaces seems to exclude models with continuous spin variables such as the XY and Heisenberg models. However, algorithms for discretized versions of these models, such as clock models, may well be feasible.

Acknowledgements

It is a pleasure to thank Prof. F.Y. Wu for his contributions to our understanding of lattice models and their phase transitions. Thanks are also due to J.R. Heringa and W. Janke for valuable discussions. This research is supported by the Dutch FOM foundation ("Stichting voor Fundamenteel Onderzoek der Materie") which is financially supported by the NWO ('Nederlandse Organisatie voor Wetenschappelijk Onderzoek').

References

[1] A.A. Belavin, A.M. Polyakov, A.B. Zamolodchikov, J. Stat. Phys. 34 (1984) 763.
[2] D. Friedan, Z. Qiu, S. Shenker, Phys. Rev. Lett. 52 (1984) 1575.
[3] J.L. Cardy, in: C. Domb, J.L. Lebowitz (Eds.), Phase Transitions and Critical Phenomena, Vol. 11, Academic Press, London, 1987, p. 55.
[4] J.L. Cardy, J. Phys. A 17 (1984) L385.
[5] J.L. Cardy, J. Phys. A 18 (1985) L757.
[6] M. Weigel, W. Janke, Europhys. Lett. 51 (2000) 578.
[7] A.A. Migdal, Zh. Eksp. Teor. Fiz. 69 (1975) 1457;
A.A. Migdal, Sov. Phys. JETP 42 (1976) 743.
[8] H.F. Trotter, Proc. Am. Math. Soc. 10 (1959) 545.
[9] M. Suzuki, Progr. Theor. Phys. 56 (1976) 1454.
[10] R.H. Swendsen, J.-S. Wang, Phys. Rev. Lett. 58 (1987) 86;
J.-S. Wang, R.H. Swendsen, Physica A 167 (1990) 565.
[11] U. Wolff, Phys. Rev. Lett. 62 (1989) 361;
U. Wolff, Phys. Lett. B 228 (1989) 379.
[12] E. Luijten, H.W.J. Blöte, Int. J. Mod. Phys. C 6 (1995) 359.
[13] P.W. Kasteleyn, C.M. Fortuin, J. Phys. Soc. Japan 26 (Suppl.) (1969) 11.
[14] H.W.J. Blöte, L.N. Shchur, A.L. Talapov, Int. J. Mod. Phys. C 10 (1999) 1137;
P. Butera, M. Comi, Phys. Rev. B 56 (1997) 8212;
R. Guida, J. Zinn-Justin, J. Phys. A 31 (1998) 8103, and references in these papers.

[15] Y. Deng, H.W.J. Blöte, Phys. Rev. E 66 (2002) 066110; and unpublished data.
[16] Y. Deng, H.W.J. Blöte, Phys. Rev. Lett. 88 (2002) 190602.
[17] T.W. Burkhardt, E. Eisenriegler, J. Phys. A 18 (1985) L83.
[18] D. Stauffer, A. Aharony, Introduction to Percolation Theory, revised 2nd Edition, Taylor&Francis, London, 1994.
[19] C.D. Lorenz, R.M. Ziff, Phys. Rev. 57 (1998) 230.